

Fatigue Strength of Self-Piercing Riveted Joints of Steel and Magnesium Alloy Sheets

¹Dong-Woon Han and ²Ho-Kyung Kim

¹Department of Automotive Engineering, Graduate School,

²Department of Mechanical and Automotive Engineering,

Seoul National University of Science and Technology, 139-743 Seoul, Republic of Korea

Abstract: Self-Piercing Riveting (SPR) process is gaining in popularity in the automotive industry. This process can be used to join similar or dissimilar materials. Application of magnesium alloy in automotive industry is increasing due to its high specific strength. Therefore, in this study, fatigue tests are performed using tensile and cross-tension specimens of magnesium alloy and steel sheets to evaluate the fatigue strength of SPR joints. For the tensile-shear and cross-tension geometries, the ratios of the fatigue endurance limit to the static strength were 26 and 9%, respectively. This indicates that the SPR joints are vulnerable to cross-tension loading, compared to tensile-shear loading. The equivalent stress intensity factor can predict the fatigue lifetimes of SPR joints with magnesium and steel sheets for the tensile-shear and cross-tension specimen geometries.

Key words: Self-piercing riveting, fatigue, tensile-shear, cross-tension, lifetimes, intensity

INTRODUCTION

Due to the urgent need to reduce fuel consumption and carbon dioxide emissions, lightweight sheet materials are being increasingly used in the automotive industry. The application of light metals such as aluminum alloy or magnesium alloy has also increased in industries. However, most of these materials are difficult or impossible to join with resistance spot welding. Friction stir welding (Uzun *et al.*, 2005), laser welding (Bassani *et al.*, 2007), SPR (He *et al.*, 2008), clinching (Kim and Kim, 2015) and adhesion (Baldan, 2004) have rapidly arisen as the main joining methods for these lightweight materials. Among these, SPR joining is widely used in the automotive industry for mainly aluminum alloys sheets. The SPR process is essentially a cold-forming operation as schematically shown in Fig. 1 in which a semi-tubular rivet is pressed by a punch into two (or more) sheets of material that are supported by a small die with a suitable geometry. A mechanical interlock is created by the rivet when it pierces the top sheet and flares in the bottom sheet under the guidance of the rivet internal geometry and the die (He *et al.*, 2008).

The fatigue strength of SPR joints has been investigated by a number of researchers for a number of materials. For example, Huang *et al.* (2017) investigated the fatigue behavior of aluminum SPR joints under tensile-shear loading. They applied a local strain-stress approach to crack initiation prediction and showed reasonable agreement in predictions of the crack initiation site. Zhang *et al.* (2017) investigated the fatigue properties of SPR joints in high-strength steel and aluminum alloy. They reported that the mechanical and fatigue performances of these two types joints were significantly influenced by the thickness and strength of the steel sheet used and were markedly improved when the thickness of the steel sheet increased. Zhang *et al.* (2016) investigated the effect of a heat treatment on the fatigue performances of SPR joints with similar and dissimilar titanium, aluminum and copper alloys. They showed that stress relief annealing had an apparent impact on the fatigue performances but had little influence on the static strengths of the joints.

The application of magnesium alloy in the automotive industry is increasing due to its high specific strength as noted above. However, investigations of the fatigue properties of SPR joints in magnesium alloys have been

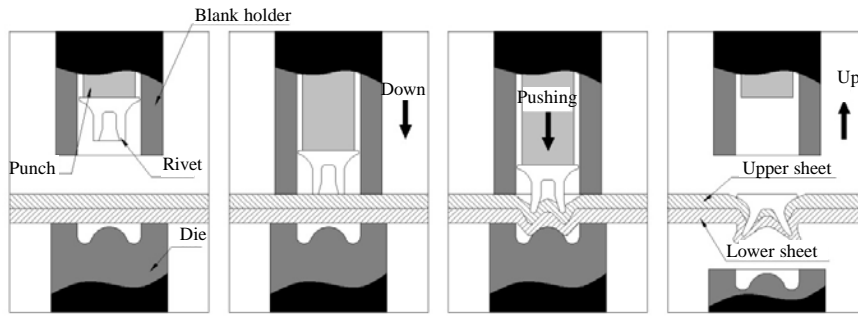


Fig. 1: An illustration of the self-piercing riveting process

limited thus far. Therefore, in this study, fatigue tests are performed using tensile and cross-tension specimens of AZ31 magnesium alloy and steel sheets to evaluate the fatigue strength of SPR joints under different loading configurations. The experimental fatigue lifetimes of SPR joint specimens are estimated using the effective stress intensity factor. The conclusions here may provide a reference for further research on SPR joints in magnesium alloys.

MATERIALS AND METHODS

In this study, an AZ31 magnesium alloy sheet and cold-rolled mild steel (SPCC) sheet with a thickness of 1.5 mm were used to create the SPR joint specimens. To evaluate the static and fatigue strengths of the SPR joints, tensile-shear and cross-tension specimens as shown in Fig. 2 were prepared. The tensile-shear and cross-tension SPR joint specimens consist of magnesium alloy as an upper sheet and steel as a lower sheet. Both the AZ31 and the SPCC sheets were cut along the rolling direction. The mechanical properties of the AZ31 and SPCC sheets are listed in Table 1.

The 0.35% carbon steel rivet used for riveting was 5.0 mm long with a diameter of 5.0 mm. A special fixture mounted onto a universal testing machine was used for the SPR joining process. Fatigue tests were conducted using a tensile-shear specimen at a load ratio $R = (P_{min}/P_{max})$ of 0.1 at a frequency of 5 Hz using a servo-hydraulic universal testing machine (Instron 8516). In order to determine the optimal riveting force, several specimens were produced using the tensile-shear specimen while the load was increased by 2~3 kN from 17-38 kN with monotonic testing used to evaluate the joint strength. The riveting force against the maximum monotonic strength for the SPR specimens is plotted in Fig. 3. The optimal riveting force was determined to be 35 kN for the specimens. Thus, all of the fatigue specimens were produced using the optimal riveting force.

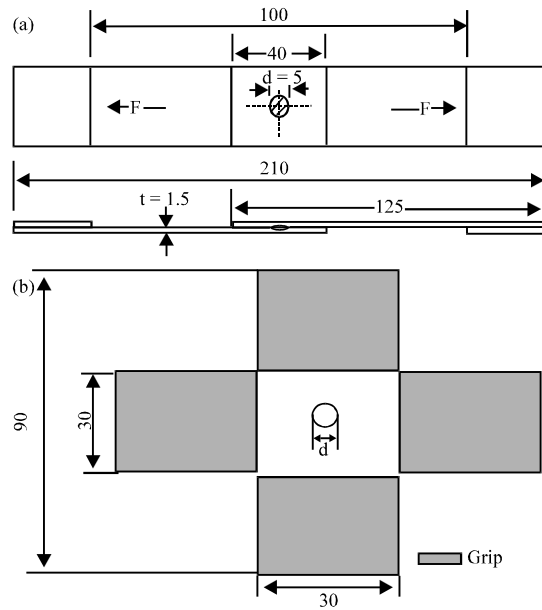


Fig. 2: Geometries and dimensions of the SPR specimens: a) Tensile-shear and b) Cross-tension

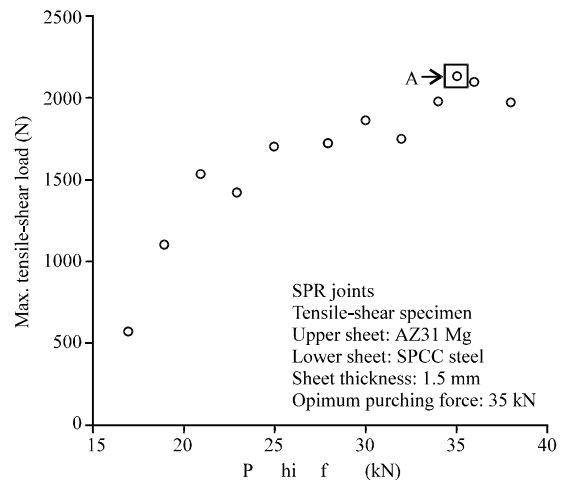


Fig. 3: Punching force against the maximum tensile-shear force of the SPR specimens

Table 1: Mechanical properties of the AZ31 and SPCC

Materials	σ_u (MPa)	σ_y (MPa)	Elong (%)
AZ31	277.7	115.8	17
SPCC	401.3	166.1	36

RESULTS AND DISCUSSION

Static strength evaluation of SPR joints: Static tests were conducted on tensile-shear and cross-tension specimens produced under the optimal riveting force. Figure 4 shows the applied load against the displacement for the tensile-shear and cross-tension specimens. The peak loads of the tensile-shear and cross-tension specimens were 3772 and 1876 N, respectively, suggesting that tensile-shear joint was stronger than the cross-tension joint. The elongation to failure of the cross-tension specimen was larger than that of the tensile-shear specimen. Both specimens fractured in the pull-out failure mode where the upper and lower sheets separated at the SPR joint.

Fatigue lifetime evaluation of SPR joints: Fatigue tests were performed on the SPR joint specimens. The fatigue failure time was defined as the instance when a crack became visible on the specimen. Figure 5 shows the load amplitude, P_{amp} ($= (P_{max} - P_{min}) / 2$), against the number of cycles to failure, N_f . The results show a relationship between the applied load amplitude and number of cycles, $P_{amp} = 4610N_f^{-0.111}$ and $P_{amp} = 1619N_f^{-0.164}$ for the tensile-shear and cross-tension specimens, respectively. The load amplitudes, corresponding to the fatigue strength at 10^6 cycles are 995 and 168 N for the tensile-shear and cross-tension specimens, respectively. The fatigue endurance of the tensile-shear specimen is higher than that of the cross-tension specimen. The fatigue ratio ($=$ ratio of endurance limit to ultimate strength) ($= 26\%$) for the tensile-shear specimen is much higher than that ($= 9\%$) of the cross-tension specimen, while its monotonic strength ($= 3772$ N) is much higher than that ($= 1876$ N) of the cross-tension specimen. This fact suggests that the fatigue performance of a magnesium-steel SPR joint is vulnerable to cross-tension loading compared to tensile-shear loading.

SPR joints generally undergo multiaxial stresses during fatigue loading. Recently, Kang and Kim (2015) attempted to predict the fatigue lifetimes of SPR joints with different specimen configurations by adopting several fatigue parameters. They showed that the equivalent Stress Intensity Factor (SIF) at a spot weld can appropriately be correlated with the fatigue lifetimes of SPR joints for various types of specimen geometries. In this study, the equivalent stress intensity factor (Zhang, 1997) was directly adopted to correlate the fatigue lifetimes of

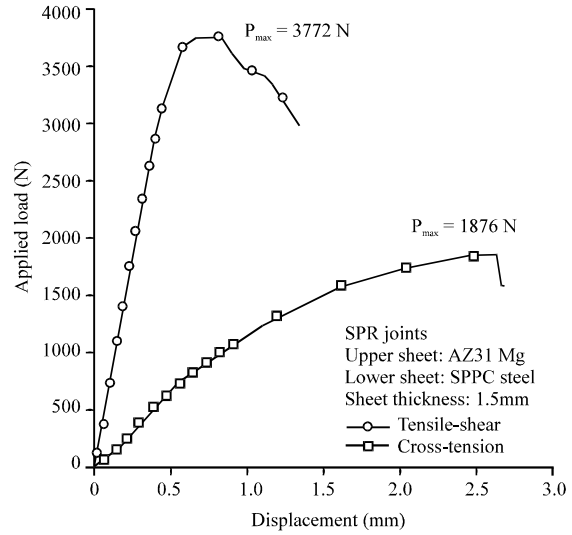


Fig. 4: Comparison of the applied load versus the displacement curves for the tensile-shear and cross-tension specimens

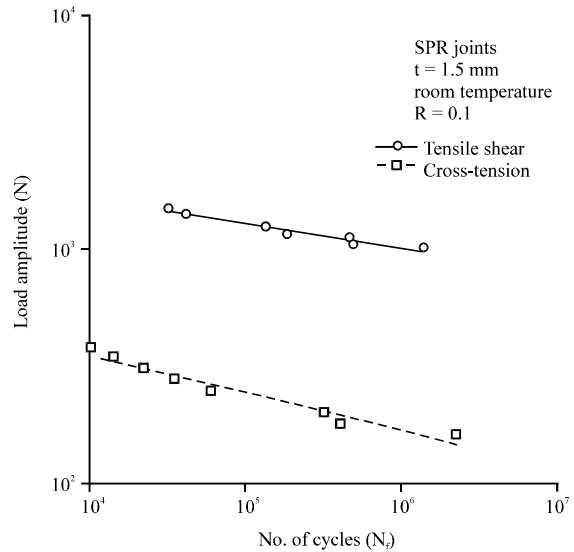


Fig. 5: Load amplitude against the number of failure cycles for SPR joints under tensile-shear and cross-tension loading

SPR joints with tensile-shear and cross-tension specimen geometries. The equivalent SIFs at a spot weld are shown as:

$$K_{eq}^{ts} = 0.694 \frac{F}{d\sqrt{t}} \tag{1}$$

$$K_{eq}^{ct} = 0.108 \frac{cF}{dt\sqrt{t}} \tag{2}$$

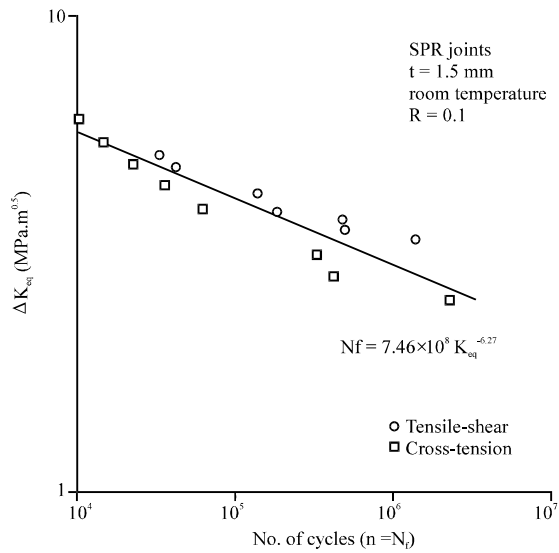


Fig. 6: Fatigue lifetimes as a function of the equivalent stress intensity factor amplitude

for the tensile-shear and cross-tension specimen geometries which have the corresponding superscript notation of ts and ct. Here, F is the applied load range, d ($= 5.0$ mm) is the rivet diameter, t ($= 1.5$ mm) denotes the specimen thickness and c ($= 30$ mm) is the load spacing as shown in Fig. 2.

Figure 6 shows the equivalent stress intensity factor against the number of cycles for the experimental fatigue lifetime of the tensile-shear and cross-tension SPR specimens. There is a relatively close relationship between the fatigue lifetimes of the tensile-shear and cross-tension specimens. The equivalent stress intensity factor is thus proved to be useful for predicting the experimental fatigue lifetime data of magnesium-steel sheet SPR joints even when the loading conditions differ.

Fatigue failure mode: The fatigue failure mode of both specimens was the interface failure mode where crack initiation occurred near the rivet between the steel and magnesium sheets and propagated through the sheet thickness. For both specimens, crack initiation occurred due to fretting between the magnesium and steel sheets. In addition, the crack started in the magnesium sheet for which the strength is lower. Figure 7a shows the interface failure mode of the tensile-shear specimen at a load amplitude of 1050 N. The crack propagated along the periphery of the rivet perpendicular to the loading direction. Figure 7b shows the interface failure mode of the cross-tension specimen at an applied load amplitude of 180 N. Fretting occurred near the triple point for the



Fig. 7: Fatigue failure specimens; a) Tensile-shear and b) Cross-tension specimens

rivet shank and the aluminum and steel sheets. The crack initiated and propagated radially into the thickness direction and then reached the final fracture state.

CONCLUSION

In this study, static and fatigue tests were conducted with tensile-shear and cross-tension specimens with AZ31 magnesium alloy and steel sheets for an evaluation of the fatigue strength of SPR joints. For the tensile-shear specimen, the optimal applied punching force for the SPR joining process was found to be 35 kN using the current sheet thickness of 1.5 mm and the geometrical dimensions of the rivet. For the tensile-shear and cross-tension geometries, the fatigue endurance limits were determined to be 995 and 168 N, respectively, assuming fatigue cycles of 10^6 for an infinite lifetime. The corresponding ratios of the fatigue endurance limit to the static strength were 26 and 9%. This indicates that SPR joints are vulnerable to cross-tension loading, compared to tensile-shear loading. Conclusively, the fatigue lifetimes of SPR joints with magnesium and steel sheets can be predicted for the tensile-shear and cross-tension specimen geometries through the equivalent stress intensity factor range.

ACKNOWLEDGEMENT

This study was financially supported by Seoul National University of Science and Technology.

REFERENCES

- Baldan, A., 2004. Adhesively-bonded joints and repairs in metallic alloys, polymers and composite materials: Adhesives, adhesion theories and surface pretreatment. *J. Mater. Sci.*, 39: 1-49.
- Bassani, P., E. Capello, D. Colombo, B. Previtali and M. Vedani, 2007. Effect of process parameters on bead properties of A359-SiC MMCs welded by laser. *Compos. Part A Appl. Sci. Manuf.*, 38: 1089-1098.
- He, X., I. Pearson and K. Young, 2008. Self-pierce riveting for sheet materials: State of the art. *J. Mater. Process. Technol.*, 199: 27-36.
- Huang, L., H. Guo, Y. Shi, S. Huang and X. Su, 2017. Fatigue behavior and modeling of self-piercing riveted joints in aluminum alloy 6111. *Intl. J. Fatigue*, 100: 274-284.
- Kang, S.H. and H.K. Kim, 2015. Fatigue strength evaluation of self-piercing riveted Al-5052 joints under different specimen configurations. *Intl. J. Fatigue*, 80: 58-68.
- Kim, J.B. and H.K. Kim, 2015. Fatigue behaviour of clinched joints in a steel sheet. *Fatigue Fract. Eng. Mater. Struct.*, 38: 661-672.
- Uzun, H., C.D. Donne, A. Argagnotto, T. Ghidini and C. Gambaro, 2005. Friction stir welding of dissimilar Al 6013-T4 to X5CrNi18-10 stainless steel. *Mater. Des.*, 26: 41-46.
- Zhang, C.Y., R.B. Gou, M. Yu, Y.J. Zhang and Y.H. Qiao *et al.*, 2017. Mechanical and fatigue properties of self-piercing riveted joints in high-strength steel and Aluminium alloy. *J. Iron Steel Res. Intl.*, 24: 214-221.
- Zhang, S., 1997. Stress intensities at spot welds. *Intl. J. Fract.*, 88: 167-185.
- Zhang, X., X. He, B. Xing, L. Zhao and Y. Lu, *et al.*, 2016. Influence of heat treatment on fatigue performances for self-piercing riveting similar and dissimilar titanium, Aluminium and copper alloys. *Mater. Des.*, 97: 108-117.